6. R. Iglish and F. Chemnitz, "On the differential equation $f''' + ff'' + \beta(1 - f'^2) = 0$ for $\beta < 0$, encountered in boundary layer theory, and for known laws of blowing and suction," in: Problems of the Boundary Layer and Heat Transfer Problems [Russian translation], Énergiya, Moscow—Leningrad (1960).
7. L. G. Loitsyanskii, Laminar Boundary Layer [in Russian], Fizmatgiz, Moscow (1962).

# DISTURBANCES OF HIGH MODES IN A SUPERSONIC JET

N. A. Zheltukhin and N. M. Terekhova

UDC 532.526.3.013.4

This article analyzes and reports the results of numerical modeling of a little-studied wavelike phenomenon seen in jet flows. Alternating light and dark bands are visible on shadowgraphs of supersonic jets flowing from circular nozzles in the underexpansion regime. These bands, present on the initial section (the first and part of the second zones), are evidence of the presence of azimuthal flow irregularities in these regions. Figure 1 [1] shows a typical Topler photograph illustrating the above. Such patterns are familiar in gasdynamics, although no explanations for them are offered either in this well-known work or in monographs on jets. Two recent experimental studies have returned to this question, the authors using different approaches in each case. The method laser diagnostics was used in [2] to study the disturbance of azimuthal symmetry for a jet discharged into a vacuum in the preturbulent regime. It was shown that the compressed layer breaks up into a certain number of lobes which are interspersed with gas from the surrounding space. This results in the formation of different transverse distributions of density $\rho$ at different azimuthal angles $\varphi$. It was suggested such an event might be a consequence of the onset of instability in the flow. The authors of [1] probed the region of the compressed layer between a suspended shock wave and the boundary of a submerged turbulent jet by traditional methods used to measure gasdynamic quantities — with a pilot tube inserted into the flow and positioned coaxially with possible streamlines. The resulting variations in total pressure indicate the existence of azimuthal irregularities of the longitudinal-velocity distributions in the region of the compressed layer. The authors stated that this is a consequence of the presence of longitudinal vorticity of the Taylor—Görtler vortex type in the flow.

The hypothesis on the wavelike nature of the observed bands is supported by experimental data obtained in the related areas of internal gasdynamics, aerodynamics, and the hydrodynamic stability of boundary flows. Here it has been possible to use visualization methods and to reliably identify the alternating bands with eddies. The genesis of these eddies may be different, however. Coherent structures in the form of stationary longitudinal vortices which are periodic with respect to the transverse coordinate (Benny—Lin vortices [3, 4]) are widely known in hydrodynamic stability. They are formed as a result of synergetic processes — the spontaneous formation of structures of a certain type of instability wave with a finite intensity. Longitudinal eddies connected with curvature of the streamlines are observed on the inside surfaces of nozzles [5], in boundary layers on concave surfaces [6], and in separated flows at sites of flow attachment [7]. Without stopping to analyze these flows in detail, it is necessary to emphasize that the turbulence mechanism noted above may also be operative in the underexpanded jet being examined here.

Thus, the initial motivation for the present investigation was to check the hypothesis of the possible existence of longitudinal vorticity in free supersonic jets in the form of stationary eddies located in the region of the compressed layer and oriented with the flow. Since the modeling will be done with incomplete information (little experimental data) and since it will therefore be impossible to unambiguously establish the origin of the vorticity, we will examine structures whose origin is related to unstable oscillations of various types.

First of all, these are waves which are steady over time and are connected with curvature of the trajectories of the gas due to the intrinsic shock-wave configuration of the

Novosibirsk. Translated from Zhurnal Prikladnoi Mekhaniki i Tekhnicheskoi Fiziki, No. 2, pp. 75-83, March-April, 1990. Original article submitted October 13, 1988; revision submitted March 9, 1989.

 0021-8944/90/3102-0232$12.50 

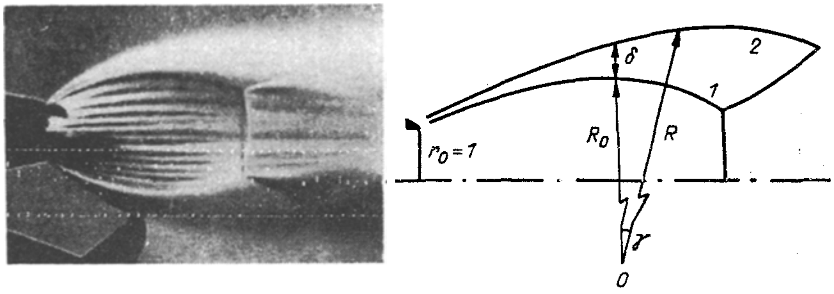


Fig. 1

nonisobaric jet. Such waves in semiinfinite flows have been referred to as Taylor–Görtler (T–G) vortices. The same term is used here for free flows, since the role of the solid wall is played by the gas of the surrounding space in the case of jets. This is evidenced by the presence of a boundary layer (mixing layer). Secondly, we are examining longitudinal eddies formed due to the nonlinear interaction of natural large-scale instability waves with the mixing layer of a jet. The interaction occurs through oscillation-induced additional forces (Reynolds stresses), i.e., they are similar in nature to Benny–Lin (B–L) vortices. We will give most of our attention to vortices of the first type, since they were examined first for jets.

Linearization of the basic equations of motion in studies of the characteristics of large-scale waves in transitional and turbulent jets is a commonly used approach which has proven effective in flows where large-scale turbulence exists in energy equilibrium with the average flow. Here, the turbulence determines the form of the mean velocities but does not have an effect on waves of a scale which is incommensurate with these velocities, i.e., does not have an effect on oscillations such as those that will be examined below.

Taylor–Görtler Vortices. The region of the compressed layer through which most of the gas flows, between the suspended shock 1 and the boundary of the jet 2 (see Fig. 1), has a complex structure. This is a region of large gradients in which the mixing layer δ is formed and where the proximity of the shock wave affects the distribution of the flow parameters. Since it is not possible to account for all of the features characterizing acceleration and deceleration of the flow, we adopted a simplified scheme which reflects the main features of the actual distributions [8] – the features that are important for analyzing waves in jets. The flow region is divided into two subregions. By analogy with an isobaric jet, the first subregion is appropriately termed the flow core. Here, the velocities and density are constant, while their derivatives are equal to zero. On a cross section, this subregion extends from the axis of the jet to the region of the compressed layer adjacent to the shock, where the changes in longitudinal velocity are small. The values of the flow parameters $\bar{W}_0$ and $\rho_0$ at its boundary are chosen as the determining parameters in the averaging of the equations. The radius of the nozzle $\bar{r}_0$ is chosen as the geometric scale. The second subregion, lying in the compressed layer, is the mixing layer. Here, velocity changes to a zero value. Analysis of the photographs and data reported in [1] shows that the transverse dimensions of these subregions within the first zone for underexpanded jets is within the range 1:(0.1-0.5). Thus, in order to be able to represent the results in a single form, we introduced one more scale factor such that for all stations downflow and all δ, the dimensionless coordinate of the half-velocity $W_0 = 0.5$ is equal to unity. Thus, the beginning of the mixing layer is determined by the value $r_1 = 1 - \delta/2$. Assigning the thickness δ should ensure a spatial error $z(\delta)$.

We will restrict ourselves to a unidimensional approximation of the field of mean velocity $\mathbf{u} = |0, 0, W_0|$. There being no data on the distribution of $W_0$ in [1, 2], we proceeded on the basis of the proposition that the longitudinal velocity $W_0$ correlates satisfactorily with the profile constructed on the basis of empirical approximations for a normally expanded jet [9]:

$$W_0(r) = \begin{cases} 1, & r < r_1, \\ \exp(-0.693\eta^2), & r \geqslant r_1, \end{cases}$$
$$\eta = (r - r_1)/(1 - r_1) \geqslant 0, \; r = 1 + \delta(\eta - 1)/2.$$

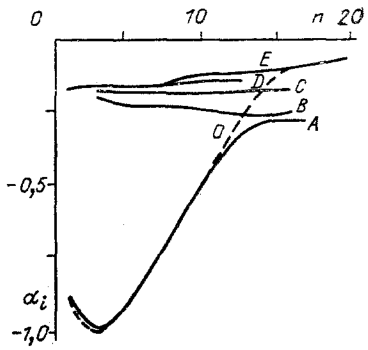


Fig. 2

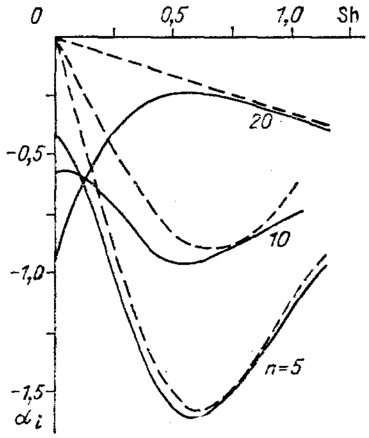


Fig. 3

Using the gasdynamic relations for an adiabatically stagnated, nonheat-conducting gas, the following relations are obtained for the density $\rho_0$ and the square of the speed of sound $a^2$ [10]:

$$\rho_0 = [1 + ((k-1)/2)M_0^2(1 - W_0^2)]^{-1},$$
$$a^2 = (\rho_0 M_0^2)^{-1},\ k = c_p/c_V,\ M_0 = \overline{W}_0/\bar{a}_0.$$

In the general case, the boundary of the jet and the suspended shock are described well by circle arcs of the radii R, $R_0 \geq 1$ with the center at a certain point O. The system r, φ, γ is chosen as the orthogonal coordinate system, where r is the radial coordinate and φ and γ are angular coordinates. The metric form in the chosen system $dS^2 = H_1^2dr^2 + H_2^2d\varphi^2 + H_3^2d\gamma^2$ (the Lamé constants $H_1 = 1$, $H_2 = R\cos\gamma - R_0$, $H_3 = R$, $R = R_0 + r$), while the velocity along the axes is designated as u, v, and w. It is evident that R changes in absolute value within the first zone, while $R_0 \gg r$. The Euler equations in (r, φ, γ) have the form

$$u_t + uu_r/H_1 + vu_\varphi/H_2 + wu_\gamma/H_3 - v^2H_{2r}/H_1H_2 - w^2H_{3r}/H_1H_3 = -p_r/\rho H_1,$$
$$v_t + uv_r/H_1 + vv_\varphi/H_2 + wv_\gamma/H_3 + uvH_{2r}/H_1H_2 + vwH_{2\gamma}/H_2H_3 = -p_\varphi/\rho H_2,$$
$$w_t + uw_r/H_1 + vw_\varphi/H_2 + ww_\gamma/H_3 + uwH_{3r}/H_1H_2 - v^2H_{2\gamma}/H_2H_3 = -p_\gamma/\rho H_3.$$

To simplify the problem, we take a section of the jet where $R_0$ can be considered constant without a large error. Thus, $\cos\gamma \approx 1$ and $\sin\gamma \approx 0$, and thickening occurs only due to an increase in δ. Then after we introduce $dz = Rd\gamma$, the system is written as

$$\begin{aligned} &u_t + uu_r + vu_\varphi/r + wu_z - v^2/r - [w^2/R_0] = -p_r/\rho, \\ &v_t + uv_r + vv_\varphi/r + wv_z + uv/r = -p_\varphi/\rho r, \\ &w_t + uw_r + vw_\varphi/r + ww_z + [uw/R_0] = -p_z/\rho. \end{aligned} \tag{1}$$

We augment it with the continuity equation

$$u\rho_r + v\rho_\varphi/r + w\rho_z + \rho(u_r + v_\varphi/r + w_z + u/r + [u/R_0]) = 0$$

and the entropy conservation equation, which is quite sufficient for wave processes

$$s_t + us_r + vs_\varphi/r + ws_z = 0$$

The additional terms associated with curvature in the longitudinal direction have been placed in square brackets. The first of them is the traditional centrifugal force. Only the first of them is manifest for a Cartesian coordinate system, the second being the analog of the Coriolis forces. The expansion of the continuity equation is connected with allowance for additional mass transfer. It has been shown numerically that all of the effects that are obtained are determined by the centrifugal term. The effect of the other two terms is very small.

The fluctuation field is established by spatially growing traveling waves:

$$\{u', v', w', \rho', p'\} = \varkappa\{iu, v, w, g, \Pi\}(r) \exp i(\tau + n\varphi), \ \tau = \alpha z - \omega t. \tag{2}$$

Here, $\alpha_r$ and n are the longitudinal and azimuthal wave numbers; $\alpha = \alpha_r + i\alpha_i$; $\alpha_r$ is the wave number; $\alpha_i$ is the growth factor; $\omega$ is the angular frequency, determining the Strouhal number $Sh = 2\pi\bar{\omega}\bar{r}_0/\bar{a}(\bar{W}_0 = 0)$; $\varkappa$ is the azimuthal parameter. Since system (1) is invariant relative to n and $\varphi$, it also describes oscillations of the standing wave type in the azimuthal direction $\varphi$. Such oscillations are obtained with the crossing of traveling waves:

$$\{u', w', \rho', p'\} = 2\varkappa\{iu, w, g, \Pi\}(r) \exp i\tau \cos n\varphi, \quad v' = 2\varkappa iv(r) \exp i\tau \sin n\varphi. \tag{3}$$

The problem of finding T–G waves consists of finding the solution of (3) with $\omega = \alpha_r = 0$:

$$w' = 2\varkappa w(r) \exp(-\alpha_i z) \cos n\varphi, \quad v' = 2\varkappa iv(r) \exp(-\alpha_i z) \sin n\varphi.$$

Linearized system (1) reduces for (2) or (3) to a single equation relative to the amplitude $\Pi$:

$$L_1(\Pi) = 0, \ L_1(\Pi) \equiv L(\Pi) + (1/R_0 + B_2 + B_3)\Pi' + [B(\alpha^2 - A_2)/A^2 + 2B_3(1/R_0 + A_1 + B_2 + B_1'/B_1)]\Pi, \tag{4}$$

where $A = \alpha W_0 - \omega$; $A_1 = 1/r - \rho_0'/\rho_0 - 2A'/A$; $A_2 = A^2/a^2 - n^2/r^2 - \alpha^2$; $B = 2B_1(W_0' + B_1)$; $B_1 = W_0/R_0$; $B_2 = B_4(B'/B - 2A'/A)$; $B_3 = \alpha B_1/A$; $B_4 = A^2/B$; the operator L describes the equation for disturbances without curvatures of the trajectories:

$$L(\Pi) = 0, \ L(\Pi) \equiv \Pi'' + A_1\Pi' + A_2\Pi. \tag{5}$$

The boundary conditions for $\Pi$ are boundedness of the disturbances in the regions of constant velocity, which makes it possible to describe them in modified Bessel functions [10].

It turns out that, compared to (5), Eq. (4) permits the existence of additional characteristic solutions which will be referred to here as branches. Branch A (Fig. 2) has the same relationship to the eigenvalues for the cylindrical wave (dashed line) that Eqs. (5) do and can thus be used to follow the effect of additional forces which arise. The remaining branches (B–E) are very conservative with respect to changes in the number of the azimuthal mode. Figure 2 shows increments of $\alpha_i$ for the frequency from the range of maximally unstable values (Sh = 0.25) for the regime $M_0 = 1.5$, $\delta = 0.15$, and $R_0 = 800$. The presence of curvature leads to an increase in the increments of the high azimuthal modes for branch A, so that for $R_0 = 25$ only modes with low azimuthal numbers n = 1-3 are close to the values of the initial relation (5). This shows that the characteristics of the main modes realized in jets at the frequency of a discrete tone are little distorted by the natural barrel-shaped flow structure, which is consistent with the good agreement between the calculations and empirical measurements of the energy-carrying frequencies.

The search for T–G waves was conducted with movement from the initial frequencies to $\omega \to 0$. For branch A (solid lines, $R_0 = 25$) and a cylindrical wave (dashed lines), this is shown in Fig. 3. The figure shows the distributions of $\alpha_i$ for different modes. As might be expected, no such disturbances exist for wave (5), i.e., only a trivial solution is possible at $\omega = 0$. The presence of the additional forces leads to manifestation of the disturbances, with their increments increasing as n increases and deviating more and more from Eqs. (5). It turns out that the additional branches may also produce stationary waves whose increments are conservative with respect to a change in frequency. The values obtained here can be extrapolated to $\omega = 0$ for sufficiently low frequencies, since (4) has a singularity in the external field when $\omega = 0$. Table 1 shows values of $\alpha$ for $R_0 = 25$ and Sh = 0.005 with branches A and D. Together with Fig. 4, these values illustrate that the characteristics of the T–G waves on branch D (line 4) are nearly the same for any n, that with an increase in n the increments of the waves from branch A tend toward asymptotes (line 1 for Sh = 0.0825), and that the actual values $\alpha_i$ for n > 20 will somewhat exceed the values reported here (line 2 for Sh = 0.005 and line 3 for Sh = 0.0025). For comparison, the table shows $\alpha_i$ for Sh = 0.0825 in accordance with Eqs. (5) (line 5). Here, it is appropriate to make certain recommendations on the experimental determination of $\alpha_i$. It is best to perform the measurements

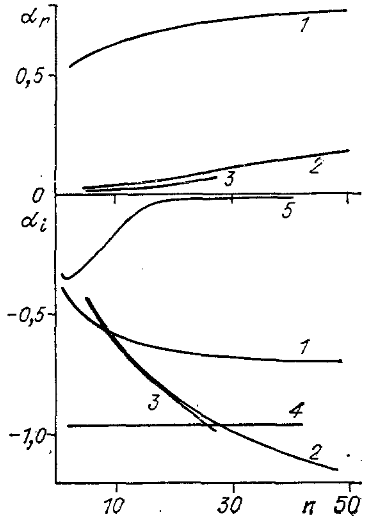


Fig. 4

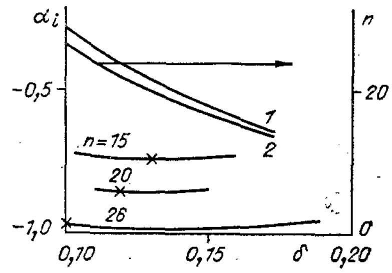


Fig. 5

TABLE 1

| n | α | |
|---|---|---|
| | branch A | branch D |
| 10 | 0,04555—0,5884i | 0,03857—0,9529i |
| 30 | 0,11471—0,9925i | 0,03835—0,9526i |
| 50 | 0,17598—1,1705i | 0,03910—0,9537i |

in several (at least two) sections that are close to each other with respect to the longitudinal coordinate z, so that the number of eddies does not change. For example, if the quantity $A_1 = A_0 \exp(-\alpha_i z_1)$ in the first section, then there is a high degree of probability that in the second section it will be written $A_2 = A_0 \exp(-\alpha_i z_2)$, from which $\alpha_i = (1/\Delta z) \ln A_2/A_1$. Measuring $A_1$ and $A_2$ and knowing $\Delta z$, we can find $\alpha_i$. Unfortunately, the interval $\Delta z$ in [1] is too large to yet permit evaluation of $\alpha_i$.

We studied the dependence of T–G waves on governing flow parameters such as δ and $M_0$. They can be linked directly with the reduction seen in [1] in the number of eddies downstream within the first zone and with the presence of a second level of accommodation noted in [2], the existence of the latter corresponding to the beginning of restructuring of the regime. The mechanism of this phenomenon is still unclear, but it can be suggested either that waves with the maximum increment are realized in the flow or that oscillations characterized by a single level of intensification survive in it. The results shown in Fig. 5 provide numerical substantiation for this hypothesis. The figure gives values of $\alpha_i$ for different modes (n = 15, 20, and 26) from branch A at Sh = 0.0025 and $R_0$ = 25. The x's denote the highest absolute values of $\alpha_i$. Meanwhile, the degree of intensification $\exp(-\alpha_i z)$ for them with regard to z(δ) [11] is roughly the same. This allows us to construct n(δ) which confirm that an increase in δ in the flow should be accompanied by a decrease in the number of vortex pairs (curves 1 and 2 for Sh = 0.005 and 0.0025), which corresponds to [1]. Due to the weakness of the dependence $\alpha_{i\,max}(\delta)$, it would be desirable to more rigorously determine the error z(δ). We found that the Mach numbers have a very slight effect on the parameters of low-frequency waves. For example, the change in $\alpha_i$ for $M_0$ = 1.5 and 4.5 was only 4%.

It was established that the T–G vortices in boundary layers next to walls are inviscid in nature [6]. We checked the effect of viscosity for a jet by introducing a correction (for viscous forces) into the right side of (4). It is evident from Fig. 6 that the changes in $\alpha_i$ for different modes from branches A and D (Sh = 0.005) are small. Thus, the conclusion regarding the weak effect of viscosity on T–G waves in the range of realistic Reynolds numbers remains valid for supersonic jets as well.

It is known that only the real parts of the solutions (4) have a physical significance. Thus, the amplitudes of the T–G waves will be $\hat{u} = -u_i$, $\hat{v} = -v_i$, $\hat{w} = w_r$, $\hat{p} = \Pi_r$, $\hat{\rho} = g_r$. Fig-

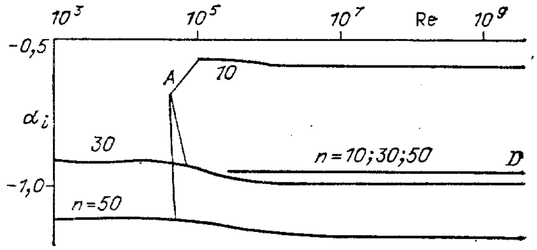


Fig. 6

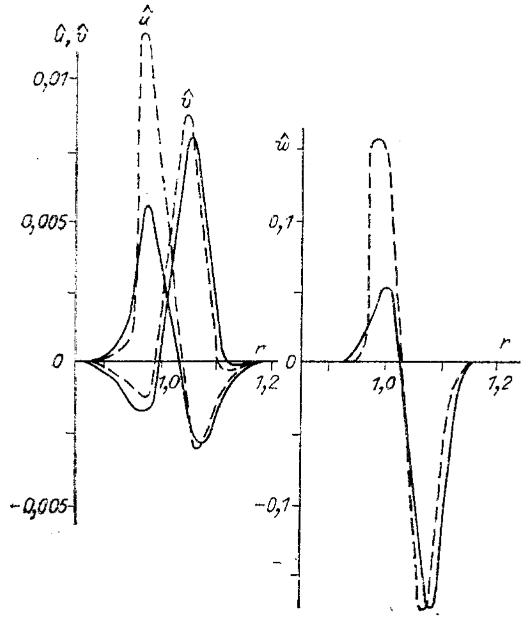


Fig. 7

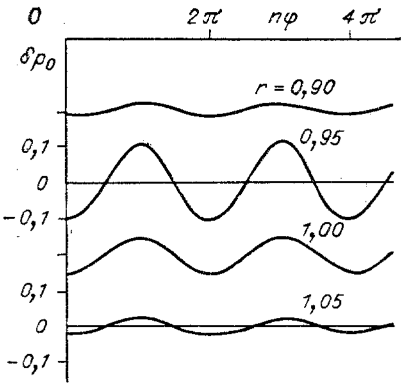


Fig. 8

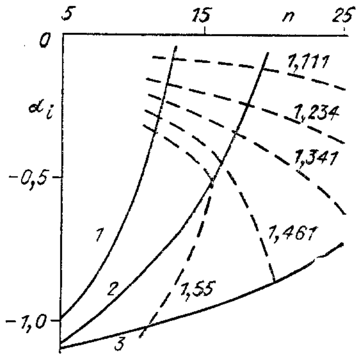


Fig. 9

ure 7 shows the amplitudes of the velocities $\hat{u}$, $\hat{v}$, $\hat{w}$ for n = 30 from branches A and D (solid and dashed lines, respectively) when they are normalized so that their maximum rms intensity $\varepsilon_t$ is 10% of the maximum mean velocity.

It should be mentioned that the velocity distributions with the additional branch turn out to be quite reasonable. Figure 8 shows transverse-azimuthal distributions of the variations of total pressure $\delta p_0$ measured in [1] for Sh = 0.0025, n = 10, $\delta$ = 0.15, and $\varepsilon_t$ = 8.6%. The following formula for the variations can be derived from the well-known gasdynamic relation for $p_0$ in [11]

$$\delta p_0 = p_0\left[\left(\frac{k-1}{k}\frac{p'}{p} + \frac{2w'}{W_0}\right)\frac{kM^2}{2+(k-1)M^2} + \frac{p'}{p}\right].$$

An analysis of this relation, accurate to within the quadratic terms, shows that $\delta p_0$ is formed mainly by the longitudinal component of the wave w' (here, $M = W_0/a$). These distributions are very similar to the experimental curves in [1], although it is difficult to compare them directly because there is no data on the most important parameters in the calculations (mainly $\alpha_i$ and $\varkappa$).

The results obtained here permit the conclusion that Taylor–Görtler vortices may be formed in actual supersonic jets.

Benny–Lin Vortices. To substantiate the possibility of the manifestation of this mechanism in a jet, it is necessary to recall the conclusions made in one of the few studies in which pulsations were measured in supersonic jets [12]. It was shown here that the rms fluctuations of mass velocity might reach 10-15%, with their distributions being adequately described by a linear approximation. As is known, B–L vortices are of the second order with respect to the amplitudes of the initial waves. Since the existence of instability waves of finite intensity in a flow is not disputed (it was not studied in [1, 2]), the above mechanism may be operative here. To exclude this as a possibility, it is necessary to show that discrete energy-carrying frequencies are absent from the amplitude-frequency spectrum.

The main aspects of the numerical modeling of vortices of the Benny–Lin type were discussed in detail in [13] for small n. Thus, here it will suffice to expand the range to large azimuthal numbers. Our study has confirmed that if instability waves of type (3) exist in a flow with an intensity great enough so that its square cannot be ignored, then these waves are capable of creating additional forces in the flow. These forces are Reynolds stresses and are determined by second-order moments. The azimuthal periodicity of the secondary flow induced by these forces will be determined by the azimuthal periodicity of the stresses $2\pi/2n$:

$$\langle u'^2\rangle = 2\varkappa^2 (u_r^2 + u_i^2)\, e^{-2\alpha_i z} \cos^2 n\varphi, \quad \langle u'v'\rangle = \varkappa^2 (u_r v_r + u_i v_i)\, e^{-2\alpha_i z} \sin 2n\varphi,$$

so that, for example, a system of 40 vortices (20 vortex pairs) can be created by waves of different modes – the mode n = 20 for T–G vortices and n = 10 for B–L vortices.

The secondary regime is studied on the basis of numerical integration of averaged equations of motion containing additional terms which connect the mean and fluctuation values of the parameters. Inclusion of additional centrifugal forces intensifies the effects that are obtained. Figure 9 shows a graph of the functions $\alpha_i(n)$ for large n and different thicknesses $\delta$ (1-3 – 0.15; 0.1; 0.05) with $M_0$ = 1.5 and Sh = 0.25. Dashes are used to show lines of equal intensification $\exp(-2\alpha_i z)$, which also makes it possible to connect the existence of growing oscillations in the flow for some thickness with the hypothesis of possible restructuring of the flow regime in accordance with the above-described scheme.

The final distributions of the amplitudes of the secondary flows and the variations of total pressure were wholly analogous to those shown in Figs. 7 and 8. They are omitted here due to the absence of error estimates for the wave parameters.

It must be emphasized once more that this qualitatively similar azimuthal distortion of the mean flow parameters is actually due to different types of oscillations having different amplitude and frequency characteristics. The exact nature of the oscillations can be established only by a special experiment. The results of the numerical modeling performed here can serve as a starting point and help determine the range of problems and parameters that needs to be addressed.

## LITERATURE CITED


1. V. I. Zapryagaev and A. V. Solotchin, "Spatial structure of the flow on the initial section of an underexpanded supersonic jet," Preprint No. 23–88, ITPM SO Akad. Nauk SSSR, Novosibirsk (1988).
2. S. A. Novopashin and A. L. Perepelkin, "Spontaneous structuring of the flow in a preturbulent supersonic jet," Preprint No. 175–88, IT SO Akad. Nauk SSSR, Novosibirsk (1988).
3. D. J. Benny and C. C. Lin, "On the secondary motion induced by oscillations in shear flow," Phys. Fluids, 3, No. 4 (1960).
4. N. A. Zheltukhin and N. M. Terekhova, "Secondary flows in an unstable boundary layer," Zh. Prikl. Mekh. Tekh. Fiz., No. 4 (1981).
5. G. F. Glotov and E. K. Moroz, "Longitudinal vortices in a supersonic flow with separated zones," Uch. Zap. TsAGI, 8, No. 4 (1977).
6. V. N. Zhigulaev and A. M. Tumin, Origin of Turbulence [in Russian], Nauka, Novosibirsk (1987).
7. A. A. Zheltovodov, E. Kh. Shilein, and V. N. Yakovlev, "Development of a turbulent boundary layer during mixed interaction with shock and rarefaction waves," Preprint No. 28–83, ITPM SO Akad. Nauk SSSR, Novosibirsk (1983).
8. V. S. Avduevskii, A. V. Ivanov, I. M. Karpman, et al., "Flow in a underexpanded viscous supersonic jet," Izv. Akad. Nauk SSSR Mekh. Zhidk. Gaza, No. 3 (1970).

9. P. J. Morris and C. K. W. Tam, "Near and far fields noise from large-scale instability of axisymmetric jets," AIAA Pap., No. 77-1351 (1977).
10. N. M. Terekhova, "Stability characteristics of a supersonic jet in a co-current flow," Izv. Sib. Otd. Akad. Nauk SSSR Ser. Tekh. Nauk, 1, No. 4 (1986).
11. G. N. Abramovich, Theory of Turbulent Jets [in Russian], Fizmatgiz, Moscow (1960).
12. G. L. Morrison and D. K. McLaughlin, "Instability of supersonic jets at low Reynolds numbers," AIAA J., 18, No. 7 (1970).
13. N. A. Zheltukhin and N. M. Terekhova, "Modeling large-scale mixing processes in an expanding supersonic jet," Zh. Prikl. Mekh. Tekh. Fiz., No. 1 (1987).

# RESONANCE FLOW RANDOMIZATION IN THE K-REGIME OF BOUNDARY-LAYER TRANSITION

S. V. Dryganets, Yu. S. Kachanov, V. Ya. Levchenko, and M. P. Ramazanov

UDC 532.536

Introduction. The empirical data presently available indicates the existence of two main regimes for the nonlinear disintegration of laminar flow in a boundary layer during the origination of turbulence. A survey of studies devoted to discovering and investigating these regimes and analyzing the reasons for their differences can be found in [1, 2]. The first regime is characterized by pulsations of characteristic bumps on the oscillograms at a certain stage of development of the instability wave. These bumps are generally regarded as corresponding to the beginning of the development of turbulence spots. This regime was first observed more than 30 yrs ago in experiments conducted at the National Bureau of Standards (USA) and was described in detail in [3]. In recognition of one of the authors of this study (Klebanov) and the fact that this regime has made an important contribution to the study of the transition to turbulence, it has been given the name "K-regime."

In 1976 investigators discovered a new, essentially different transition regime not characterized by the above-mentioned bumps or any of the other features associated with the K-regime [4]. The transition to turbulence in this regime occurred through a fairly smooth increase in the higher harmonics of the main instability wave, the appearance of a broad packet of low-frequency pulsations in the spectrum (including the subharmonic of the main wave), and their subsequent interaction and filling of the entire spectrum [4] (also see [5]).

The existence of two main transition regimes was confirmed by visualization of the perturbation field in a boundary layer in [6, 7]. It was shown in [8] that one regime is replaced by the other. Soon afterward [9, 10], it was explained that the main mechanism responsible for the development of a three-dimensional flow and randomization of the flow in the new transition regime is subharmonic parametric resonance of the plane main wave (of frequency $\omega_1$) and three-dimensional stochastic background pulsations of the broad continuous spectrum within the region of the frequency of the subharmonic $\omega_{1/2} = \omega_1/2$. A mathematical model of this interaction in a triplet (low-mode) approximation was first proposed in [11, 12]. A weakly linear theory of the formation of the new regime which quantitatively describes experimental observations was constructed in [13, 14]. Due to the determining role of subharmonic parametric resonances in the new type of transition, this type of disintegration of laminar flow is usually referred to in the literature as the "subharmonic" regime.

However, in accordance with the resonance-wave concept of disintegration proposed in [1, 2] and confirmed directly in [15], parametric resonances of the subharmonic type also play the main role in the formation of the K-regime bumps. However, in this case we are dealing not with a single resonance, but with a system of resonances which intensifies deterministic initiating waves that are coherent with the main wave. In light of this, the term "subharmonic" can be used with the same (or even greater) degree of justification in regard to the K-regime of transition. Its use to denote a new regime is very unfortunate.

---

Novosibirsk. Translated from Zhurnal Prikladnoi Mekhaniki i Tekhnicheskoi Fiziki, No. 2, pp. 83-94, March-April, 1990. Original article submitted January 18, 1989.

0021-8944/90/3102-0239$12.50 